PNAS RESEARCH ARTICLE | MEDICAL SCIENCES OPEN ACCESS

Inhaled *DNAI1* mRNA therapy for treatment of primary ciliary dyskinesia

Mirko Hennig[a,1], Rumpa B. Bhattacharjee[a,1], Ishita Agarwal[a], Ali Alfaifi[a], Jade E. Casillas[a], Sofia Chavez[a], Daniella Ishimaru[a], David Liston[a], Sakya Mohapatra[a], Touhidul Molla[a], Suyog Pathare[a], Maninder S. Sidhu[a], Peng Wang[a], Zechen Wang[a], T. Noelle Lombana[a,2], Vladimir G. Kharitonov[a], Jessica A. Couch[a], David J. Lockhart[a,2], and Brandon A. Wustman[a]

Affiliations are included on p. 11.

Edited by Brigid Hogan, Duke University Medical Center, Durham, NC; received October 25, 2024; accepted March 11, 2025

Primary ciliary dyskinesia (PCD) is an autosomal recessive disorder caused by mutations in one of at least 50 different genes that encode proteins involved in the biogenesis, structure, or function of motile cilia. Genetically inherited defects in motile cilia cause PCD, a debilitating respiratory disease for which there is no approved therapy. The dynein axonemal intermediate chain 1 (DNAI1) protein is a key structural element of the ciliary outer dynein arm (ODA) critical for normal ciliary activity and subsequent clearance of mucus from the conducting airways in humans. Loss-of-function mutations in DNAI1 account for up to 10% of all PCD cases, with functional abnormalities in patients presenting at or near birth and leading to a life-long course of disability, including progressive loss of lung function and bronchiectasis by adulthood. This underscores the significant unmet need for disease-modifying treatments that restore ciliary activity and mucociliary clearance in PCD patients. In this work, we demonstrate that lipid nanoparticle (LNP)-formulated human *DNAI1* mRNA can be delivered as an aerosol to primary human bronchial epithelial cell models and to nonhuman primate (NHP) lungs. Additionally, we show that delivery of aerosolized LNP-*DNAI1* mRNA to NHPs leads to detectable levels of newly translated human DNAI1 protein, at doses that overlap with exposures in an in vitro cell-based PCD model enabling rescue of ciliary function. Therefore, these data support further development of the inhaled *DNAI1* mRNA therapy in clinical studies as a potential disease-modifying treatment for PCD.

primary ciliary dyskinesia | dynein axonemal intermediate chain 1 | mRNA therapy | lipid nanoparticle | aerosol

Significance

Primary ciliary dyskinesia (PCD) is caused by loss of ciliary activity and mucociliary clearance, resulting in recurrent respiratory tract infections and bronchiectasis, with no disease-modifying therapies available. We demonstrate that delivery of mRNA, encoding the entire dynein axonemal intermediate chain 1 (DNAI1) protein, can rescue ciliary activity in a PCD in vitro cell model. In nonhuman primates (NHPs), aerosolized delivery of lipid nanoparticle (LNP)-formulated D*NAI1* mRNA at doses sufficient to detect newly translated human DNAI1 protein in cilia was also shown to rescue ciliary function in in vitro PCD models. Thus, these data support further development of the mRNA therapy currently in clinical development for the treatment of PCD.

Human airways and contiguous structures, such as the nasopharynx, paranasal sinuses, and middle ear are lined by ciliated, pseudostratified columnar epithelium. Continuous and coordinated beating of cilia at a particular frequency transports the mucus layer toward the oral cavity (1, 2). This coordinated movement confers the body's mucociliary clearance defense system and constitutively clears pathogens and other foreign material trapped in the mucus out of the airways (3, 4).

Primary ciliary dyskinesia (PCD), an autosomal recessive genetic disorder, affects the body's ability to clear mucus due to mutations in one out of at least 50 different genes encoding proteins involved in the biogenesis, structure, or function of motile cilia (5). Clinical manifestations include neonatal respiratory distress, situs abnormalities, and chronic infections of the upper and lower respiratory tracts (LRTs) leading to sinusitis, bronchiectasis, and sometimes respiratory failure. The minimum global prevalence of PCD is estimated to be at least 1 in 7,554 individuals (6); however, this is likely an underestimation as variants of uncertain significance may be disease-causing and some pathogenic variants in the Genome Aggregation Database may have been undetectable with current analysis methods (6).

DNAI1 was the first pathogenic gene identified for PCD in 1999 (7). The DNAI1 protein is a key structural element of the ciliary outer dynein arm (ODA) critical for normal ciliary activity and subsequent clearance of mucus from the conducting airways in humans (8–10). The ODAs are complex motors, consisting of multimers of light, intermediate, and heavy chains, required for ciliary function (11). Mutations in DNAI1 can disrupt the assembly of ODA complexes, including heterodimers formed by DNAI1 and dynein axonemal intermediate chain 2 (DNAI2), leading to impaired or more commonly, a total loss of ciliary activity.

To date, there are no approved therapies that address the underlying cause of PCD, only medications that provide palliative symptomatic relief. Thus, there is a significant unmet need for disease-modifying treatments that restore ciliary activity and mucociliary

Author contributions: M.H., R.B.B., D.I., D.L., V.G.K., D.J.L., and B.A.W. designed research; R.B.B., I.A., A.A., J.E.C., S.C., S.M., T.M., S.P., M.S.S., P.W., and Z.W. performed research; M.H., R.B.B., D.I., D.L., T.N.L., J.A.C., and B.A.W. analyzed data; and M.H., R.B.B., T.N.L., D.J.L., and B.A.W. wrote the paper.

Competing interest statement: All authors were employees at ReCode Therapeutics, Inc when data was generated.

This article is a PNAS Direct Submission.

[1]M.H. and R.B.B. contributed equally to this work.

[2]To whom correspondence may be addressed. Email: nlombana@recodetx.com or dlockhart@recodetx.com.

This article contains supporting information online at https://www.pnas.org/lookup/suppl/doi:10.1073/pnas.2421915122/-/DCSupplemental.

Published April 28, 2025.

clearance in this patient population. Because PCD is heterogeneous with over 50 validated genes causing disease when mutated, drug development is challenging as it requires targeting subpopulations, gene by gene. Recent advances in oligonucleotide-based therapies, gene therapy, and gene editing technologies have provided hope that these modalities may successfully restore ciliary function in these PCD patient subpopulations (5, 12, 13). While some founder mutations have been identified in the dynein axonemal intermediate chain 1 (*DNAI1*) gene (14), other pathogenic mutations also occur throughout the gene. Here, we describe a mutation agnostic mRNA-based potential therapeutic approach for the treatment of PCD caused by pathogenic mutations in the *DNAI1* gene, where *DNAI1* mRNA is encapsulated in a Selective Organ Targeting (SORT) lipid nanoparticle (LNP) formulation and delivered as an inhaled aerosol. SORT LNPs are five-component LNPs that were initially developed for intravenous delivery of mRNA to specific organs (15), and the formulation used in this study was optimized for aerosol delivery to lung epithelial cells and compatibility with nebulization. Therefore, this mRNA-based approach holds the promise to be readily expandable to PCD patients suffering from mutations in genes other than *DNAI1*, once an efficient delivery platform is established.

In this study, SORT LNPs carrying sequence optimized *DNAI1* mRNA are successfully delivered as an aerosol to respiratory epithelial cells in vitro and in vivo. This results in expression of wild-type, exogenous DNAI1 protein, and incorporation within the ciliary axoneme. Additionally, rescued ciliary motility is observed in an in vitro PCD human disease model representative of loss of function mutations via *DNAI1* knockdown in primary human bronchial epithelial cells (hBECs). This in vitro model has been shown to produce all the relevant respiratory epithelial cell types, form tight junctions, produce mucus, and demonstrate coordinated ciliary transport. Grown at an air–liquid interface (ALI), hBECs mimic the apical surface of airways and have been successfully used in drug development to generate personalized medicines for the related disease indication of cystic fibrosis (16). *DNAI1* mRNA administered via inhalation to nonhuman primates (NHPs) results in DNAI1 protein expression in the targeted lung cell types, ciliated, club, and basal cells. Moreover, we used experimentally determined aerodynamic particle size distributions (APSD) and delivered doses (DD) in conjunction with the multiple-path particle dosimetry (MPPD, version 3.04) (17, 18) software to simulate and compare inhaled aerosol deposition patterns in NHPs to exposures used in vitro. Importantly, doses sufficient to detect newly translated human DNAI1 protein in NHPs overlapped with exposures used to rescue ciliary function in the PCD DNAI1 knockdown hBEC model. These data suggest that an inhaled *DNAI1* mRNA gene therapy could address the underlying cause of PCD for patients harboring *DNAI1* mutations.

Results

Development of an in vitro Human PCD Cell Model. For a robust human PCD knockdown lung epithelial cell model, we first demonstrated that wildtype (WT) primary hBECs could differentiate into all relevant cell types (*SI Appendix*, Fig. S1*A*). Flow cytometry in conjunction with immunofluorescence (IF) using a set of cell-type specific markers (acetylated α-tubulin (AT) for ciliated cells, club cell 10 kD protein (CC10) for club cells, mucin 5AC (MUC5AC) for goblet cells and cytokeratin-5 (KRT5) for basal cells) demonstrated hBEC differentiation into relevant lung epithelial cell subsets, with observed ranges of 53.6% to 64.3% basal cells, 11.3% to 12.9% club cells, 24.2% to 36.1% ciliated cells, and ≤1.0% goblet cells (*SI Appendix*, Figs. S1*B* and S2). Next, we established that normal ciliated surfaces were maintained in cell culture. Mean ciliary active area (percentage of culture surface area with motile, beating cilia) of 15 batches of WT hBEC cultures, as determined by high-speed Sisson-Ammons Video Analysis (SAVA) (19) was 61% ± 12%, with a corresponding average ciliary beat frequency (CBF) of 11.6 ± 1.0 Hz (*SI Appendix*, Fig. S3), consistent with reported ranges of 5 to 15 Hz (20–22). Additionally, ciliary activity of WT hBEC cultures grown at ALI reached a plateau around 4 wk, when cultures can be considered well-differentiated, and can be maintained for almost 2 mo (56 d) (*SI Appendix*, Fig. S4). Thus, primary WT hBECs can propagate into ciliated cell precursors (basal and club cells) and ciliated cells with normal CBF.

To knockdown (KD) the expression of DNAI1 in primary WT hBECs, a commercially available lentiviral vector encoding a small hairpin (sh)RNA targeting *DNAI1* and puromycin cell resistance that enabled selection of transduced cells was used. To compare ciliogenesis and ODA assembly in WT and DNAI1-KD hBEC cultures, the levels of DNAI1 and dynein axonemal intermediate chain 2 (DNAI2) proteins, that form ODA preassembly complexes in the cytoplasm during ciliogenesis, were analyzed by WB. In vitro studies have shown that the cytoplasmic assembly factor ZMYND10 is required to stabilize DNAI1, which in turn stabilizes DNAI2 (23). This is consistent with observations in nasal epithelial cell cultures derived from patients with pathogenic DNAI1 mutations, which also completely lack DNAI2 protein (24). As expected, endogenous DNAI1 and DNAI2 protein levels in the WT hBEC cultures increased during ciliogenesis between days 12 and 22, while DNAI1-KD hBEC cultures lacked or showed reduced levels of DNAI1 and DNAI2, respectively (Fig. 1 *A-B*). To detect the absence or presence of DNAI1 in the axoneme, cultures were fixed after dosing with LNP-formulated *DNAI1* mRNA and permeabilized with Triton X-100 prior to fixation to remove cytoplasmic DNAI1 protein while leaving axonemal DNAI1 protein intact (Fig. 1*C*). Axonemal DNAI1-HA protein was detected by IF colocalization using anti-HA and AT antibodies. The conserved distribution of ciliated cells between WT DNAI1 and DNAI1-KD hBECs seen by IF confirmed that the lentiviral transduction did not interfere with normal differentiation of ciliated cells. Moreover, significantly reduced DNAI1 protein levels were detected in DNAI1-KD hBECs compared to WT hBECs (Fig. 1*C*). Importantly, DNAI1-KD hBECs recapitulated the biochemical and functional defects (e.g., loss of area showing detectable ciliary beating) seen in the airways of PCD patients with pathogenic mutations in *DNAI1* (Fig. 1*D*) thereby establishing a representative PCD lung epithelial cell model to use for DNAI1 protein incorporation and rescue experiments.

LNP-Formulated *DNAI1* mRNA Delivery to DNAI1-KD hBEC Cultures Results in DNAI1 Protein Expression and Incorporation into the Ciliary Axoneme. To understand the overall transfection efficiency as well as epithelial cell subtypes targeted by our SORT LNP formulation, we added a C-terminal hemagglutinin (HA) tag to human DNAI1 to enable detection of newly translated DNAI1 protein and differentiate from any endogenously made DNAI1 protein present due to incomplete knockdown. Two routes of LNP-formulated *DNAI1-HA* mRNA administration were compared: 1) aerosol delivery using a Vitrocell exposure chamber in conjunction with an Aerogen Solo mesh nebulizer and 2) basolateral delivery where LNP-formulated *DNAI1-HA* mRNA was added to the culture medium. hBEC cultures transfected by aerosol delivery or basolateral delivery were incubated for 5 h or 4 h, respectively, prior to harvesting 24 h posttreatment for analysis. Nebulized in vitro doses were converted to μg/cm^2 by

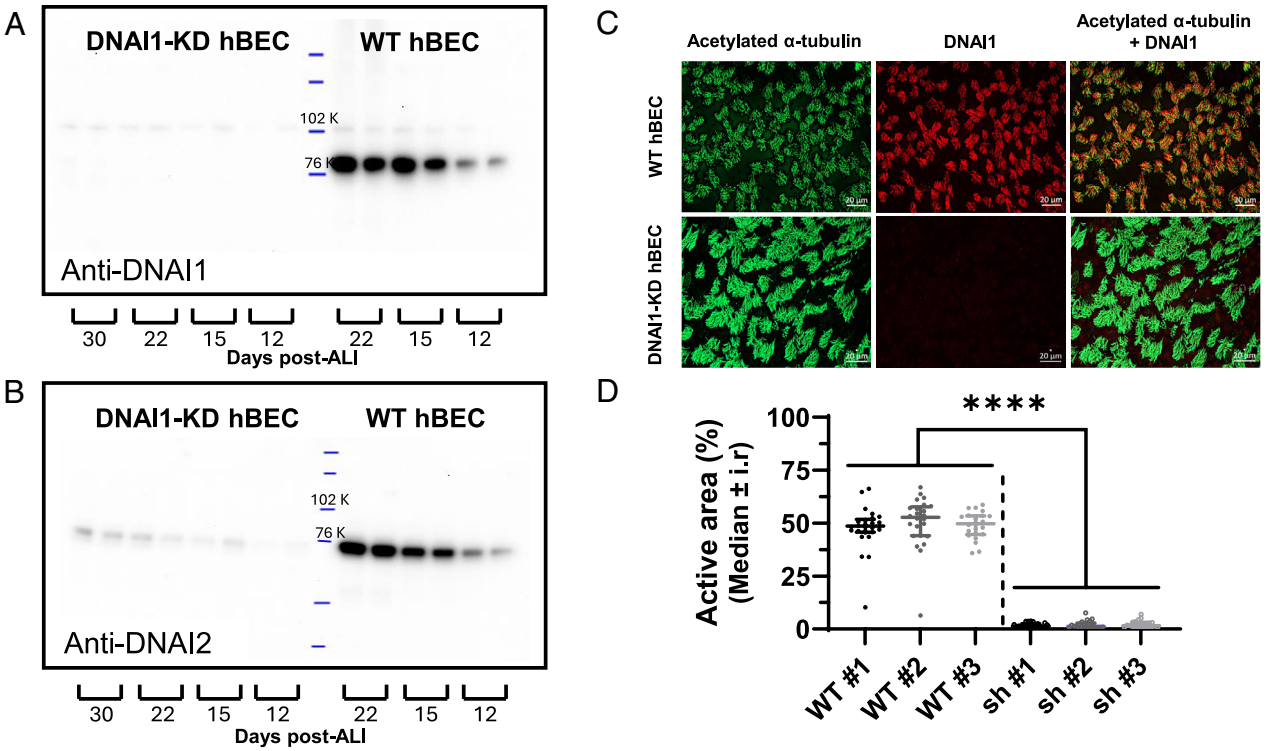

Fig. 1. Comparison of DNAI1 protein expression and ciliary activity in DNAI1-KD and WT hBEC cultures. Western blot (WB) analysis probing (*A*) DNAI1 or (*B*) DNAI2 shows protein levels are undetectable or reduced, respectively, in DNAI1-KD hBECs at all timepoints (days post-ALI) assessed during differentiation compared to WT hBEC cultures, where DNAI1 and DNAI2 levels increase during differentiation. The reduction of DNAI2 levels in DNAI1-KD hBECs is consistent with reports that DNAI2 protein is absent in cells derived from patients with mutations in *DNAI1*. (*C*) Well-differentiated (33-d post-ALI) WT and DNAI1-KD hBECs immunostained with anti-acetylated α-tubulin antibodies (green) for ciliated cells and anti-DNAI1 antibodies (red). While ciliated cells in WT hBECs colocalized with DNAI1 (yellow), only nonspecific DNAI1 protein staining at background levels was detected in DNAI1-KD hBECs. (Scale bar, 20 μm.) (*D*) WT hBEC controls (untransduced) and WT hBEC transduced with shRNA (DNAI1-KD) were grown at an ALI for 31 d under puromycin selection. Ciliary activity was measured using high-speed video microscopy and SAVA software with each dot representing percent active area of a given FoV and data represented as median with corresponding ranges. ****$P \leq 0.0001$, one-way ANOVA.

assuming even distribution of 300 μL of aerosol droplets at a concentration of 1 μg/μL onto the 138.9 cm^2 surface area of a Vitrocell exposure chamber and a growth area of 1.12 cm^2 per Transwell (TW) insert. The overall fractional aerosol deposition on the bottom of the exposure chamber was assumed to be 85% (25) where losses can mainly be attributed to condensation on the chamber walls. For example, aerosol administration in vitro leads to estimated exposures of 1.9 μg/cm^2 per 300 μL of LNP-formulated *DNAI1-HA* mRNA nebulized at a concentration of 1 μg/μL. For basolateral delivery, 20 μg/mL in 1.5 mL of medium can translate to a maximum exposure of 26.8 μg/cm^2 assuming complete delivery through the porous 1.12 cm^2 membrane of TW inserts during a 4 h incubation. Compared to basolateral delivery, single-treatment, nebulized delivery has limitations of deliverable volume (≤ 500 μL) and LNP concentration (≤1 μg/μL) which restricts dosing ranges achievable.

As anticipated, basolateral delivery of LNP-formulated *DNAI1-HA* mRNA led to higher transfection efficiencies of WT hBEC cultures in vitro based on HA-positive cells (12.4%) when compared to single-dose, aerosol delivery (0.8%) of LNP-formulated *DNAI1* mRNA (*SI Appendix*, Fig. S5). After a single, basolateral dose of *DNAI1-HA* mRNA to WT hBEC cultures and subsequent DNAI1-HA translation measured by the number of HA-positive cells, flow cytometric analysis identified preferential transfection of basal cells (~92% basal cells within DNAI1-HA positive cells). Interestingly, within the DNAI1-HA positive cells, a noticeable fraction of ciliated cells at the apical surface was observed (11% ciliated cells within DNAI1-HA positive cells), while only ~2% of HA-positive cells were club cells (*SI Appendix*, Figs. S6*A* and S7*B*). A single aerosol delivery to the apical surface of WT hBEC cultures revealed well-distributed delivery to target cell populations, including ciliated (15% ciliated cells within DNAI1-HA positive cells) as well as progenitor club (42% club cells within DNAI1-HA positive cells) and basal cell (26% of DNAI1-HA positive cells) subpopulations (*SI Appendix*, Figs. S6 *B* and S7 *B* and *C*).

Using the DNAI1-KD hBEC culture PCD in vitro model system, we demonstrated that *DNAI1-HA* mRNA encapsulated in a SORT LNP formulation and delivered via nebulization using a Vitrocell exposure chamber led to effective translation of DNAI1-HA protein in a dose-dependent manner as monitored by WB 24 h posttreatment (Fig. 2*A*). IF imaging further demonstrated that newly translated DNAI1-HA protein was incorporated into the ciliary axoneme (Fig. 2*B*), and that the colocalization of DNAI1-HA protein with acetylated-tubulin increased in a statistically significant, dose-dependent manner observed after two nebulization treatments (Fig. 2*C*).

To qualitatively assess the DNAI1-HA protein turnover after incorporation into the axoneme of cilia, well-differentiated DNAI1-KD hBEC cultures were treated with a single treatment of LNP-formulated *DNAI1-HA* mRNA (10 μg/mL in medium) from the basolateral side. Two treated inserts were fixed for each time point (1, 2, 7, 14, and 24 d posttreatment) and time-dependent incorporation of DNAI1-HA protein into the ciliary axoneme was detected by IF colocalization. DNAI1-HA protein incorporated into the axoneme of cilia was observed as early as 24 h (1 d) and persisted to the longest time point assessed (24 d posttreatment) (Fig. 3*A*). Accumulation and distribution of DNAI1-HA

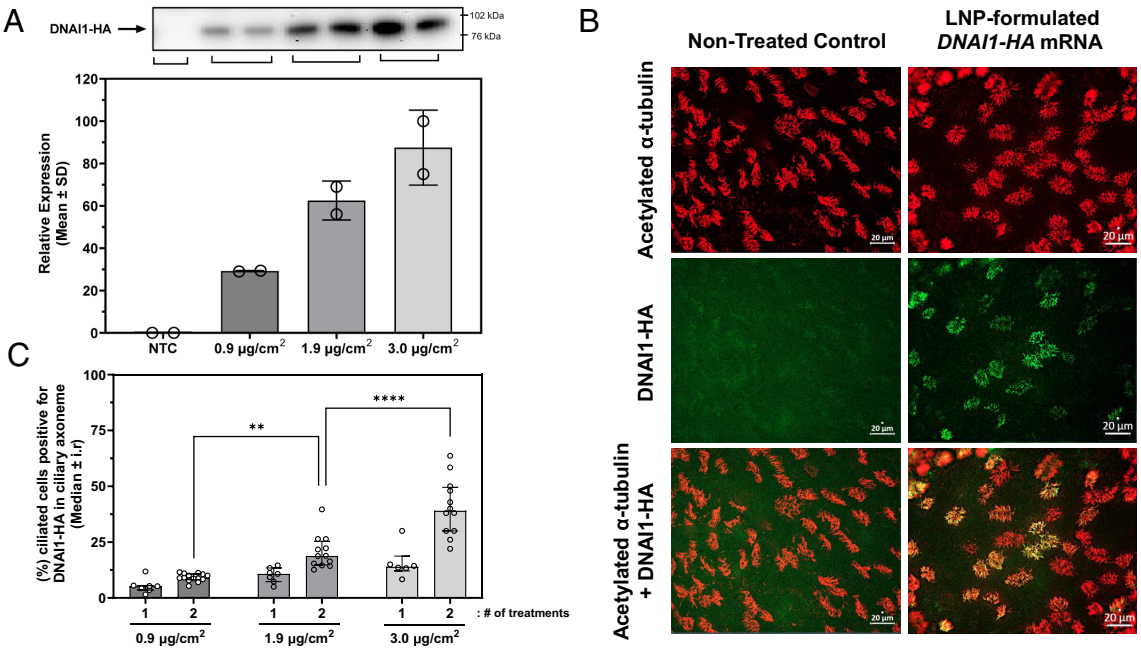

Fig. 2. Incorporation of DNAI1-HA protein into the axoneme of ciliated cells by nebulization. (*A*) Well-differentiated DNAI1-KD hBEC cultures (33-d post-ALI) were treated with a single nebulization of 0.9, 1.9, or 3.0 µg/cm^2 of LNP-formulated *DNAI1-HA* mRNA. For WB analysis, cultures were harvested 24 h posttreatment. NTC: Nontreated control. (*B*) Well-differentiated DNAI1-KD hBEC cultures (33-d post-ALI) were treated with two nebulizations of 1.9 µg/cm^2 of LNP-formulated *DNAI1-HA* mRNA on two consecutive days. Immunofluorescence (IF) showing DNAI1-HA protein (HA tag, green) in ciliated cells (acetylated α-tubulin protein in ciliary axonemes, red) and their colocalization (yellow) in treated DNAI1-KD hBEC cultures, while nontreated control shows no DNAI1-HA protein or colocalization with ciliary axoneme. Cytoplasmic signals were eliminated by permeabilization using a Triton wash prior to fixation to improve axonemal imaging. (Scale bar, 20 µm.) (*C*) Well-differentiated DNAI1-KD hBEC cultures (33-d post-ALI) were treated with one or two nebulization treatments of 0.9 µg/cm^2, 1.9 µg/cm^2, or 3.0 µg/cm^2 of LNP-formulated *DNAI1-HA* mRNA. The number of ciliated cells (acetylated α-tubulin) with colocalized DNAI1-HA (HA-tag) was divided by the total number of ciliated cells and multiplied times 100 to calculate the percentage of ciliated cells with DNAI1-HA protein in the ciliary axoneme. **$P \leq 0.01$, ****$P \leq 0.0001$, one-way ANOVA.

protein incorporation into ciliary axonemes using aerosol delivery was explored by administering LNP-formulated *DNAI1-HA* mRNA up to three times per week (1.9 µg/cm^2 per treatment) to well-differentiated DNAI1-KD hBEC cultures. Twenty-four hours after one aerosol treatment, newly expressed DNAI1-HA protein was enriched in the proximal region, whereas after 72 h, DNAI1 appeared to be distributed over the entire length of ciliary axonemes (Fig. 3*B*). After three treatments, we observed a statistically significant increase in the % of ciliated cells with incorporation of DNAI1-HA protein into ciliary axonemes as compared to a single treatment, demonstrating accumulation of DNAI1 protein with repeated nebulization (Fig. 3*C*).

Together, these data demonstrate that LNP-formulated *DNAI1* mRNA delivered by aerosol or by basolateral administration can be translated into protein and integrated into the human ciliary axoneme, where it can be detected for an extended duration (up to 24 d) following a single delivery. Furthermore, the number of ciliated cells that incorporated newly translated DNAI1 protein into ciliary axonemes showed a dose-dependent response indicating that increasing dose and frequency of administration would likely increase the number of ciliated cells of PCD patients expressing exogenous, WT DNAI1 protein. We next asked whether exogenous DNAI1 mRNA delivered to the in vitro hBEC culture PCD model would be able to restore ciliary motility.

Repeated Delivery of LNP-Formulated *DNAI1* mRNA onto DNAI1-KD hBEC Cultures Rescues Ciliary Activity. To assess whether recurrent delivery of LNP-formulated *DNAI1* mRNA by nebulization can restore ciliary motility in DNAI1-KD hBEC cultures, well-differentiated cultures were treated with the equivalent of 1.9 µg/cm^2 of *DNAI1* mRNA using a Vitrocell exposure chamber equipped with an Aerogen® Solo nebulizer. Aerosol administrations were repeated twice weekly on consecutive days for 3 consecutive weeks. Nebulized *tdTomato* mRNA treatment of DNAI1-KD hBEC cultures using identical LNP composition and dose constituted the control group. In DNAI1-KD hBEC cultures, ciliary activity is significantly reduced compared to WT hBEC cultures (Figs. 1*D* and 4*A*). An increase in active ciliary surface area was observed within a week following two nebulizations of LNP-*DNAI1-HA* mRNA and continued to increase with recurrent treatments compared to control cultures. It should be noted that all treated cultures showed an increase in background ciliary activity over time, likely a result of the waning effect of the shRNA-mediated *DNAI1* knockdown. Due to the background level of ciliary activity, the CBF for the DNAI1-HA treated groups were characterized only using the fields of view (FoV) with % active areas above the highest measured in control cultures (>29%). These FoV had CBF values ranging from 6 to 9 Hz (Fig. 4*B*) and overlapped with the ranges observed in WT hBEC cultures (*SI Appendix,* Fig. S3*B*), suggesting that translated DNAI1 protein is functional and can restore ciliary activity. Additionally, repeated nebulization treatments of 0.9 and 1.9 µg/cm^2 LNP-formulated *DNAI1* mRNA delivered 3 times a week for 3 wk to WT hBECs were shown to be well tolerated (*SI Appendix,* Fig. S8).

To confirm ciliary rescue is occurring in mature dysfunctional cilia, well-differentiated DNAI1-KD hBEC cultures (22 d post-ALI) were treated basolaterally with a 10 µg/mL dose of LNP-formulated *DNAI1* mRNA in 500 µL of medium in 0.3 cm^2 Falcon inserts (16.7 µg/cm^2 maximum exposure assuming complete delivery through the porous membrane within 4 h of incubation). After five treatments (3 per week), the DNAI1-KD hBEC cultures had significantly increased motile ciliary area when compared to the *tdTomato* mRNA treated control cultures (*SI Appendix,*

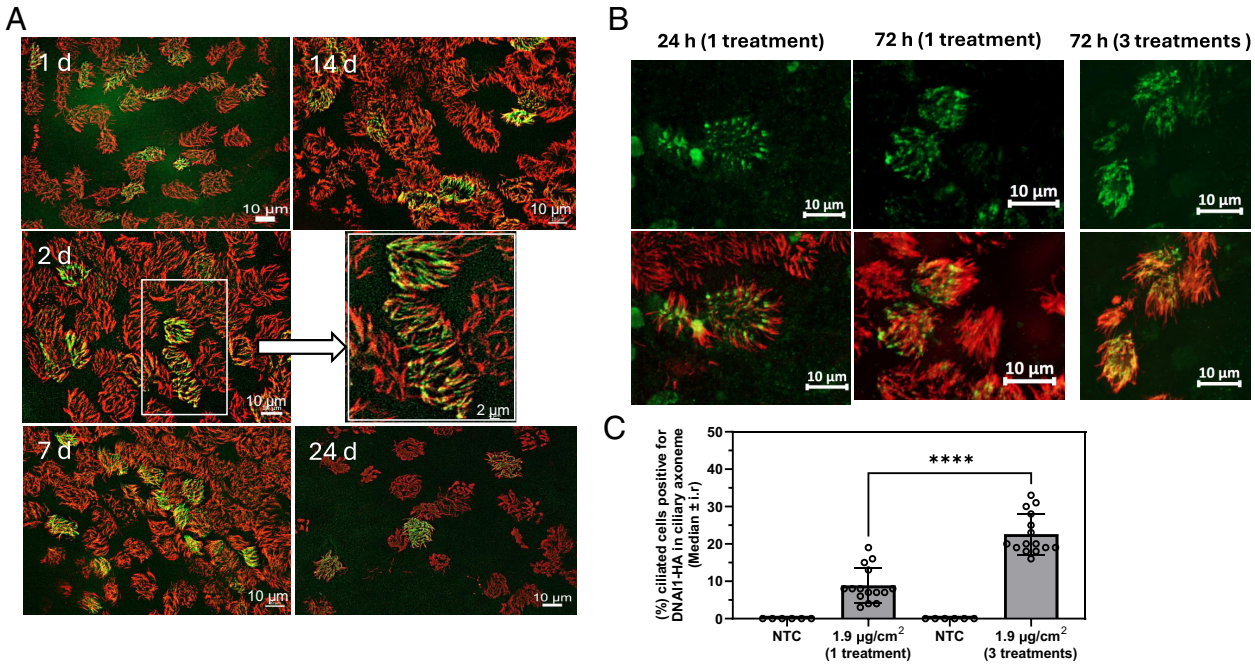

Fig. 3. Durable and dose-dependent incorporation of DNAI1-HA protein into the axoneme of ciliated cells. (*A*) Well-differentiated DNAI1-KD hBEC cultures were treated once with LNP-formulated *DNAI1-HA* mRNA by addition to the basolateral medium (10 µg/mL). Medium containing formulation was replaced with fresh medium after 5 h. Treated inserts were fixed using 4% paraformaldehyde at different days posttreatment (1 d, 2 d, 7 d, 14 d, and 24 d). IF images show localization of cilia in red (acetylated α-tubulin), DNAI1-HA in green (HA-tag), and DNAI1-HA protein colocalization with cilia in yellow. Cytoplasmic signals were eliminated by permeabilization using a Triton wash prior to fixation to improve axonemal imaging. (*B*) Well-differentiated DNAI1-KD hBEC cultures (31 d post-ALI) were treated with one or three aerosol administrations of 1.9 µg/cm^2 of LNP-formulated *DNAI1-HA* mRNA. Cytoplasmic signals were eliminated by permeabilization using a Triton wash prior to fixation to improve axonemal imaging. Inserts were fixed at 24 or 72 h post–single treatments and 72 h post–three treatments and IF images use the same markers as in Panel *A*. (*C*) The number of ciliated cells (stained with acetylated α-tubulin) with colocalized DNAI1-HA (HA-tag) detected 72 h after 1 or 3 treatments from Panel *B* was plotted as a percentage of the total number of ciliated cells to show the incorporation of DNAI1-HA in the ciliary axoneme. NTC: nontreated control. ****$P \leq 0.0001$, one-way ANOVA.

Fig. S9*A*). Last, to understand whether ciliary rescue is also occurring during ciliogenesis, differentiating DNAI1-KD hBEC cultures (12 d post-ALI) were treated repeatedly from the basolateral side by addition of 10 µg/mL LNP-formulated *DNAI1*. Although the differentiating DNAI1-KD hBEC cultures feature fewer ciliated cells when compared to well-differentiated cultures (*SI Appendix,* Fig. S4), five basolateral treatments (3 per week) of LNP-formulated *DNAI1* mRNA significantly increased active areas compared to the control cultures treated with *tdTomato* mRNA (*SI Appendix,* Fig. S9*B*).

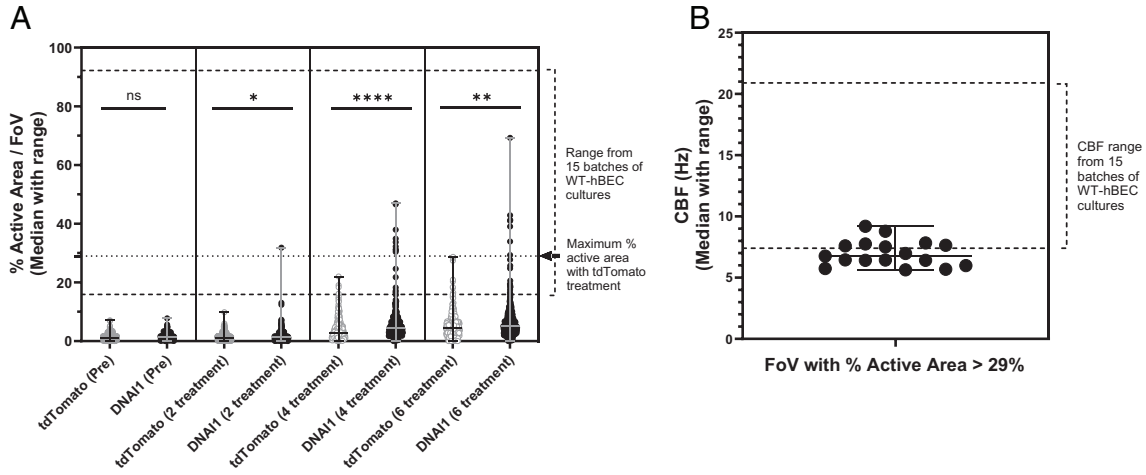

Fig. 4. Functional rescue of ciliary activity in DNAI1-KD hBEC cultures by treatment with nebulized LNP-formulated *DNAI1* mRNA. Well-differentiated DNAI1-KD hBEC cultures (44-d post-ALI) were treated with two nebulizations of 1.9 µg/cm^2 of LNP-formulated *DNAI1-HA* mRNA or LNP-formulated *tdTomato* mRNA on two consecutive days each week for up to three weeks. (*A*) Ciliary activity in hBEC cultures was recorded and analyzed by SAVA software to yield a ciliary % active area score for approximately 350 individual, nonoverlapping fields of view (FoV) per insert. Two inserts were scored per treatment group. Ciliary % active area ranges observed in WT hBEC cultures (*SI Appendix,* Fig. S3*A*) are highlighted using dashed lines. The FoV showing maximum % active area for control, *tdTomato* mRNA treated cultures is indicated using a dotted line. *DNAI1* mRNA treated cultures have higher levels of ciliary activity after 2, 4, and 6 treatments as compared to *tdTomato* mRNA treated cultures. Increased activities were statistically significant as determined by Welch's *t* test. *$P < 0.05$, **$P = 0.001$, ****$P < 0.0001$, ns = not significant ($P > 0.05$). (*B*) Ciliary beat frequencies for *DNAI1* mRNA treated cultures. FoV with % active areas >29% (those with % active areas greater than that observed in any *tdTomato* mRNA treated cultures) overlap with the WT hBEC culture CBF range of 7.4 to 20.9 Hz (*SI Appendix,* Fig. S3*B*) and fall within the normal reported CBF literature range of 5 to 15 Hz.

These data confirm that administration of LNP-formulated *DNAI1* mRNA results in expression of functional, wildtype DNAI1 protein that can restore ciliary activity in vitro. Robust ciliary activity characterized by CBF within normal ranges can be restored using either nebulized or basolateral delivery routes and rescue can occur in both differentiating cells undergoing ciliogenesis and in differentiated cells with mature cilia. Next, we examined whether DNAI1-HA protein could be translated in relevant respiratory cell types after inhaled delivery of LNP-formulated *DNAI1* mRNA in vivo.

Biodistribution Evaluation in Cynomolgus Monkeys after LNP-Formulated *DNAI1* mRNA Intubated Aerosol Delivery. LNP-formulated *DNAI1* mRNA was studied in vivo in NHPs to evaluate the biodistribution in the lung and its potential to induce expression of DNAI1 protein in lung cell types relevant to PCD. Specifically, ventilated cynomolgus monkeys (*Macaca fascicularis*) were administered a single 0.51 mg/kg dose by inhaled, intubated delivery of LNP-formulated *DNAI1-HA* mRNA or a vehicle control (buffer only). No animal had adverse reactions and no significant change in body temperature or weight was observed postexposure or up to 6 h thereafter (*SI Appendix*, Fig. S10). Again, we used DNAI1-HA to enable detection of newly translated human DNAI1 protein following LNP-formulated delivery and to differentiate it from endogenously made NHP DNAI1 protein, as the human and cynomolgus monkey DNAI1 protein homologs are ~95% identical. A respiratory tissue sample was collected from the trachea (below the intratracheal tube cuff) and bronchi in two NHPs (one/sex) at 6 h postdose and examined by multiplex immunofluorescence (mIF) to identify newly made, human DNAI1-HA protein. In addition, four lung tissue samples representing large and small conducting airways and alveoli were collected from each NHP. The highest expression levels of DNAI1-HA protein in the respiratory tissues after a single administration were found in the bronchi compared to the trachea tissue revealing an average (n = 2) of 7.29% versus 2.41% HA-positive cells, respectively, and an average (n = 8) of 1.63% of total cells were HA-positive in the lung sections (Fig. 5 *A*–*C*). From the total of all cells counted, ranging from 592,909 to 1,198,084, the assay background as determined by the vehicle control group (two NHPs; one/sex) was 0.04% HA-positive cells. In the trachea, bronchi, and lung sections, DNAI1-HA protein could be delivered via intubation to epithelial, ciliated, club, basal, and goblet cells (Fig. 5 *A*–*C*). DNAI1-HA epithelial expression was detected by costaining with epithelial cellular adhesion molecule (EpCAM) antibody and the average (N = 2) percentage of DNAI1-HA positive epithelial cells were 10.5% in bronchi, 3.5% in lung, and 2.9% in trachea tissue samples (Fig. 5 *A*–*C*). The highest expression levels of DNAI1-HA protein were seen in club cells for all tissues and an increase in DNAI1-HA protein levels detected in ciliated cells after LNP-formulation *DNAI1-HA* mRNA treatment was seen in the trachea and lung sections. In the bronchial section, the percentage of DNAI1-HA positive cells detected for each cell type were 13.1% of ciliated cells, 20.6% of club cells, 7.5% of basal cells and 7.1% of goblet cells. A similar ranking was observed for the lung samples. Importantly, cell tropism patterns

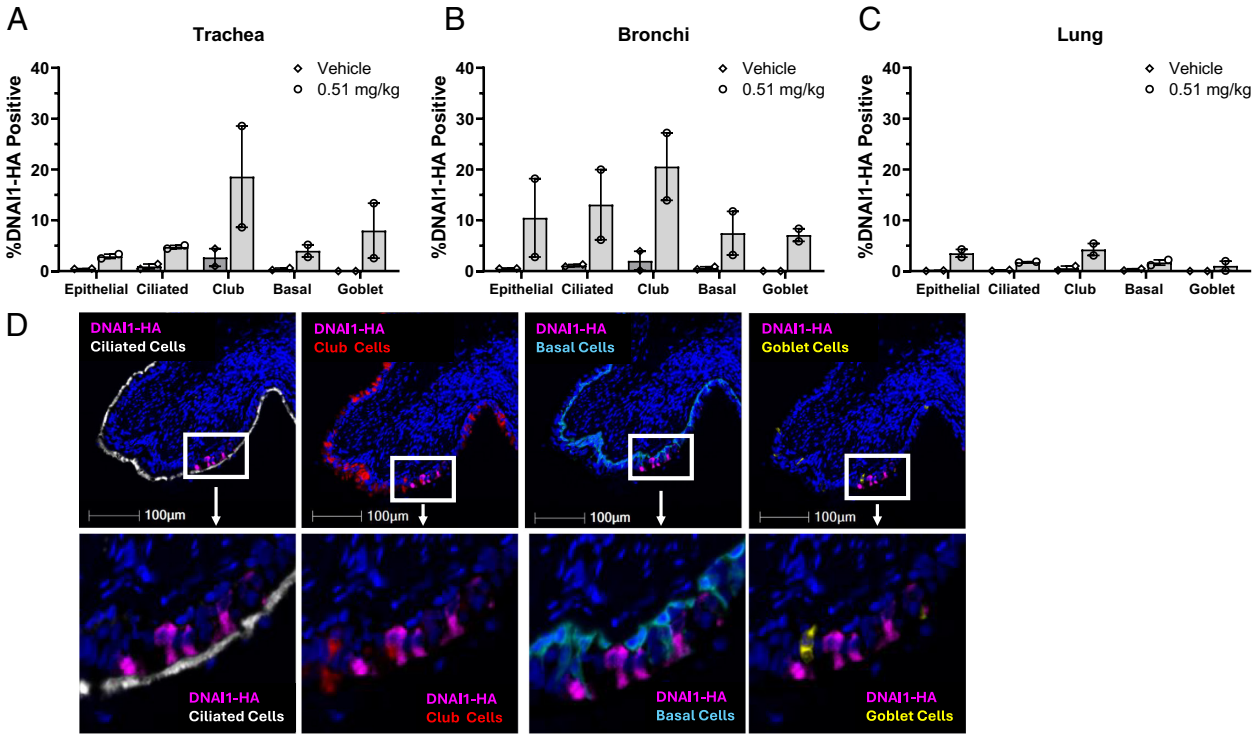

Fig. 5. Newly made DNAI1-HA protein observation in target cells in NHP lungs after inhaled, intubated delivery of LNP-formulated *DNAI1-HA* mRNA. Following a single 0.51 mg/kg administration of inhaled (intubated) LNP-formulated *DNAI1-HA* mRNA or vehicle (buffer only) lung, bronchial and tracheal sections were collected from two NHPs (one per sex) 6 h after dosing. Multiplex immunofluorescence (mIF) was used to quantitate cells that had colocalization of DNAI1-HA (using HA-tag marker) with other respiratory cell types (using cell-specific markers: EpCAM for epithelial cells, acetylated tubulin for ciliated cells, CC10 for club cells, cytokeratin 5 for basal cells, and mucin 5AC for goblet cells. (*A*–*C*) Shown are the individual data points for each treated animal and the mean ± SD dev. for each group (n = 2). The % DNAI1-HA positive population for each cell type was calculated from (*A*) a single stained tracheal section per animal with total cell count range of ~30,000 to 42,000, (*B*) a single stained bronchial section per animal with total cell count range of ~18,000 to 22,000, or (*C*) four stained lung sections per animal with total cell count range of ~72,000 to 397,000. (*D*) Representative mIF images from a section of respiratory epithelium demonstrating a cluster of DNAI1-HA positive cells using HA marker (magenta; see arrows) along with individual cell-type markers of acetylated tubulin for ciliated cells (white), CC10 for club cells (red), cytokeratin 5 for basal cells (light green), and mucin 5AC for goblet cells (yellow). The *Top* panels have a scale bar of 100 µm and a further zoomed version of the white boxes are shown in the *Bottom* panels for more clarity.

Table 1. Summary of model parameters used in NHP respiratory MPPD modeling

	Intubated NHP, LNP-*DNAI1-HA* @ 0.5 mg/mL
Lung morphology	
Airway model	Rhesus symmetric, <BW> = 3.07 ± 0.18 kg
FRC (functional residual capacity)	137.3 mL
URT (upper respiratory tract)	5.27 mL
Surface area of the tracheo-bronchiolar region	704 cm^2
Generation 0 to 8 (Trachea + B ronchi + Bronchioles)	26 cm^2
Generation 9 to 15 (Bronchioles)	678 cm^2
Surface area of the alveolar region	79,775 cm^2
Droplet properties of LNP-*DNAI1* using Aerogen Solo	Aerodynamic Particle Sizer (APS)
MMAD (mass median aerodynamic diameter)	1.95 μm
GSD (geometric SD)	1.77
Exposure conditions	
Body orientation	On left side
Breathing frequency	30 per minute
Tidal volume	41.0 mL
Inspiratory fraction	0.35
Breathing scenario	Endotracheal

observed in vivo are similar to those observed in vitro when the DNAI1-HA mRNA is delivered to WT-hBECs via nebulization (*SI Appendix*, Fig. S6*B*). Fig. 5*D* shows representative mIF images from an NHP lung section containing respiratory epithelium, illustrating a cluster of human DNAI1-HA positive cells along with ciliated, club, goblet, or basal cells. As expected due to the 6-h timepoint of this experiment, the in vitro DNAI1-HA protein is mainly observed in the cytoplasm, whereas the early stages of ciliary incorporation are observed at ~24 h (Fig. 3 and *SI Appendix*, Fig. S11).

In summary, DNAI1-HA expression was confirmed in target cell populations relevant to PCD pathophysiology, including ciliated cells and their precursors, basal and club cells. Based on these data, we next used computational modeling to predict whether the NHP lung exposures of LNP-formulated *DNAI1* mRNA were sufficient to rescue ciliary activity.

Simulation of Inhaled Aerosol Deposition Patterns in NHP Lungs. Obtaining regional deposition patterns for lungs directly through in vivo experiments in animal models is challenging. Instead, computational simulation based on mathematical models of aerosol droplet transport and deposition within the airway may provide better insight into in vivo-in vitro dose translations (26). The MPPD (version 3.04) software was employed in this study to simulate inhaled aerosol deposition patterns in NHPs (17, 18). It should be noted that this modeling does not take into consideration how excess mucus in the airways of PCD patients may impact distribution and efficiency of mRNA delivery nor does the computational approach simulate deposition in a cell-type specific manner. Besides the geometry model of the NHP LRT, the MPPD-based inhalation exposure assessment requires properties of mass median aerodynamic diameter (MMAD) and geometric standard deviation (GSD) for the intubated exposure scenarios. Experimentally derived aerosol properties (MMAD and GSD) and exposure conditions employed to administer a single 0.51 mg/kg dose by inhaled delivery of LNP-formulated *DNAI1-HA* mRNA are summarized in Table 1 and were used with the symmetric Rhesus airway morphometry model and the average body weights (BW) $<BW_{intubated}>$ = 3.07 ± 0.18 kg) to predict particle deposition fraction in the respiratory tracts of NHPs (Table 2). Simulated regional deposition fractions are governed by diffusion, inertial impaction, and gravitational settling revealing local maxima at generation 6, 15, and 20 (*SI Appendix*, Fig. S12*A*). The MPPD model utilizes a rhesus monkey lung LRT geometry model developed using computed tomography (CT) images of the tracheobronchial (TB) airways of a 6-mo-old male NHP to construct a conducting airway tree together with computed morphometric data from the literature to construct the alveolar region geometry (18). Simulations can be extended over a wide range of body weights and ages for both sexes by rescaling lung surface areas (summarized in Table 1 and shown in *SI Appendix*, Fig. S12*B*) and usage of adapted age-specific values of lung and breathing parameters. Here, MPPD calculations were done using a functional residual capacity (FRC) of 137.3 mL and upper respiratory tract (URT) volume of 5.27 mL. The breathing frequency (BF) was set to 30 breaths/minute, the tidal volume (TV) to 10 to 15 mL/kg of NHP body weight and a 35:65 inspiratory to expiratory ratio was used. Airway morphometry data in NHP, such as FRC, URT volume, BF, and TV, are summarized in Table 1.

During intubated exposures, the LNP-formulated *DNAI1-HA* mRNA containing aerosol had a MMAD of 1.95 μm with a GSD of 1.77. Bypassing the head via tracheal intubation, approximately one third (34.6%) of the droplets deposit in the tracheobronchial (TB) region, while the remaining 19.8% of inhaled droplets deposit in the pulmonary (P) region (Table 2 and Fig. 6*A*). In intubated animals, generations 1-9 comprising bronchi and bronchioles are predicted to be exposed to more than 1.9 $μg/cm^2$ of nebulized LNP-formulated *DNAI1-HA* mRNA (Fig. 6*B*), which

Table 2. Predicted deposition patterns in NHP using the Rhesus symmetric airway model

Target region	Intubated, NHP ($t_{exposure}$ ≤ 30 min)
Total (%)	53.5
Head (%)	–
TB (%)	33.6
P (%)	19.9
Exposures	
Total (mg/kg)	0.51
Head ($μg/cm^2$)	n.d.*
TB ($μg/cm^2$)	0.75
Trachea + bronchi + bronchi-oles (generations 0 to 8) ($μg/cm^2$)	14.68
Bronchioles (generations 9 to 15) ($μg/cm^2$)	0.21
Alveoli (generations 16 to 23) ($μg/cm^2$)	0.0039

*n.d.: Not determined.

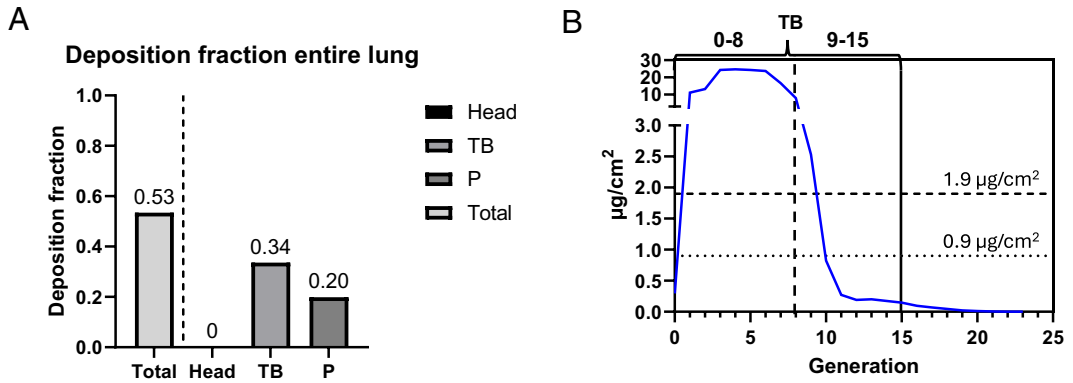

Fig. 6. Simulated deposition distribution for intubated NHP using experimentally determined aerosol characteristics. (*A*) Multiple-path particle dosimetry (MPPD)-simulated deposition fractions using symmetric Rhesus airway morphometry model in NHP Head (head airway), TB (tracheobronchial), P (pulmonary), or Total (sum of Head, TB, and P) lung regions using intubated exposure (see Table 1 for simulation inputs and Table 2 for numerical results). (*B*) Exposure levels as a function of generation # reached in the entire lung region (generations 0-23) following LNP-formulated *DNAI1* mRNA administration to intubated (blue line) NHP. The dashed horizontal line (1.9 µm/cm^2) represents exposure levels sufficient to rescue ciliary activity in a cell-based model. The dotted horizontal line (0.9 µm/cm^2) represents exposure levels sufficient to detect newly expressed DNAI1-HA in a cell-based model. A vertical dashed line separates conducting airways of the TB region composed of generations 0 to 8 (trachea + bronchi + bronchioles) and 9 to 15 (bronchioles).

was sufficient to rescue ciliary activity in vitro. Predicted depositions are less than 0.1 µg/cm^2 outside the TB region, starting at generation 16.

Discussion

A DNAI1 knock-out mouse model has been described in the literature (Dnaic1 knockout) (27), however, while these mice suffer from rhinosinusitis, this model does not develop the lung phenotype observed in PCD patients that underlies much of the disease-associated morbidity. Therefore, to evaluate the therapeutic potential of LNP-encapsulated *DNAI1* mRNA, we developed a human in vitro PCD model using shRNA to knockdown *DNAI1* gene expression in primary hBECs (DNAI1-KD). hBEC cultures are considered the most appropriate human airway cell model available given that these primary human cultures reproducibly recapitulate several key features of the respiratory epithelium, including relevant cell types (basal, ciliated, and secretory cells) and cellular characteristics (tight gap junctions, synchronized ciliary activity, mucus secretion). In addition, hBECs cultured at the ALI have been used for the successful development of new therapies for CF (28–30).

Using a DNAI1-KD hBEC-based in vitro PCD model, we established functional ciliary rescue with surface areas showing detectable ciliary motility and CBF within normal ranges after treatment with SORT LNP-formulated *DNAI1* mRNA. Rescue was seen in both differentiating (treatment starting at 12 d post-ALI) as well as well-differentiated (treatment starting between 21 and 44 d post-ALI) DNAI1-KD hBEC cultures. Furthermore, ciliary activity was rescued in DNAI1-KD hBEC cultures repeatedly exposed to SORT LNP-formulated *DNAI1* mRNA delivered either basolaterally or as an aerosol. Irrespective of route of administration (basolateral or nebulization) or timing of treatment (in differentiating or differentiated hBECs), robust ciliary functional rescue was achieved. Together with the observed maturation of lung cells in the in vitro model where ciliated cell populations increased during ciliogenesis and reached a plateau at approximately 4 wk, we suggest that rescue of ciliary motility can occur through direct transfection of ciliated cells.

Of note, the lowest dose sufficient to rescue ciliary activity in our in vitro PCD model is difficult to establish due to limitations of the in vitro model system (i.e., based on transient viral knockdown of *DNAI1*) and the nebulization route via Vitrocell exposure chambers (i.e., feasible volume and concentration of LNP-formulated *DNAI1* mRNA for consistency in aerosolization). In experiments conducted to date, 1.9 µg/cm^2 was the lowest dose tested that could be successfully distinguished from background levels of activity in the DNAI1-KD hBEC cultures. However, in vitro exposures of 0.9 µg/cm^2 are sufficient to detect newly expressed DNAI1-HA protein in the ciliary axoneme. Additionally, a single administration of LNP-formulated *DNAI1-HA* was shown to rapidly incorporate and distribute throughout the cilia within 24 and 48 h of treatment, respectively, where it remained detectable for more than 3 wk. In our studies with hBEC cultures, the number of ciliated cells positive for DNAI1-HA in their cilia accumulated with increasing dose or number of treatments. While the half-life of human ciliated cells within the epithelium is impacted by many variables including age, health, and injury, the turnover rate of the ciliated epithelium is thought to be generally slow (1 to 4 mo) (31). Taking this into account, our results suggest that repeat dosing with exposures explored in these studies, could lead to an accumulation of rescued function over time within the ciliary fields of the pulmonary epithelium.

Inhaled delivery enables direct access to the airway epithelium, a key site of disease relevance for the treatment of PCD, without many of the inefficiencies or unwanted effects that can be associated with systemic drug delivery. To estimate how DD between in vitro and in vivo models translate, the MPPD v3.04 software was used to estimate lung deposition in intubated NHPs. Intubated delivery to anesthetized NHPs is tightly controlled with tidal volumes, breathing frequencies, and inspiratory to expiratory ratios dialed into the respirator. The delivery times are short (typically ≤ 30 min) and endotracheal breathing scenarios provide useful models better mimicking human delivery through nebulizer fitted mouthpieces while avoiding extensive aerosol deposition in the URT of treated humans. Estimated NHP exposures are within the range of exposures needed to enable translation of functional DNAI1 protein and rescue of ciliary function after multiple dose administration in vitro. Predicted exposures also overlap with exposures shown to be sufficient to detect newly translated DNAI1 protein in target cells of the NHP lung after delivery via inhalation. Importantly, ciliated cells are not uniformly distributed over the epithelial surface and abundance decreases in a proximal to distal direction (i.e., trachea > bronchi > bronchioles > terminal bronchioles > pulmonary airways). This identifies the tracheobronchial as opposed to the pulmonary region as an optimal target region for

LNP-formulated *DNAI1* mRNA inhaled delivery to maximize uptake in ciliated cells and their precursors (32).

In summary, we describe an mRNA-based therapeutic in clinical development intended to rescue a genetic deficit in PCD caused by pathogenic mutations in the *DNAI1* gene. As an integral part of the ciliary ODA structure, the DNAI1 protein is critical for normal human ciliary function and subsequent clearance of mucus from the conducting airways. Our data suggest that improving human ciliary function is possible with inhaled delivery of SORT LNP-formulated *DNAI1* mRNA to the PCD target cells of the respiratory epithelium, including ciliated, club and basal cells, and subsequent translation to functional DNAI1 protein. Thus, aerosol delivery of LNP-formulated *DNAI1* mRNA to PCD DNAI1 patients is proposed to improve mucociliary clearance and these data support the further development of the *DNAI1* mRNA therapy as a disease-modifying treatment for PCD.

Materials and Methods

mRNA Production. DNA plasmids containing polyA-tailed and sequence-optimized [hemagglutinin (HA)-tagged and untagged)] *DNAI1* mRNA coding for the canonical human DNAI1 protein (Uniprot: Q9UI46-1) were enzymatically linearized. All mRNA constructs were generated using DNA-template directed in vitro transcription using T7-RNA polymerase with N1-methyl-pseudouridine ($m^1\psi$) triphosphate substitution for naturally occurring uridine triphosphate. In vitro transcriptions were performed following standard conditions. Posttranscriptional enzymatic 5′-capping was performed as described by the manufacturer (New England Biolabs #M2080S). 5′-capped *DNAI1* mRNA samples were then purified and resuspended in water. Subsequently, mRNA samples were passed through a 0.22 μm filter and stored frozen at -80 °C until they were formulated.

Lipid Nanoparticle Formulation. *DNAI1* mRNA-loaded SORT-LNPs were prepared via nanoprecipitation by mixing *DNAI1* mRNA in an aqueous buffer (sodium citrate buffer, pH 4.0) and an organic (ethanol) solvent stream containing an ionizable lipid (15, 33), a cationic SORT lipid (1,2-dimyristoyl-sn-glycero-3-ethylphosphocholine), 1,2-dioleoyl-sn-glycero-3-phosphoethanolamine (DOPE), cholesterol, and 1,2-di myristoyl-rac-glycero-3-methoxypolyethylene glycol-2000 (DMG PEG2k) in a volumetric flow ratio of 3:1. The initially formed LNPs are allowed to anneal at room temperature for 30 min. After the annealing step, the LNPs are diluted with water in a volume ratio of approximately 1:1, resulting in diluted LNPs. This step is performed to further reduce the level of ethanol in the mixture. The diluted LNP produced is subjected to buffer exchange either using a desalting column or by tangential flow filtration (TFF) in a crossflow system with a buffer containing 15 mM Tris, 10% sucrose (%w/v), pH 7.5. The buffer exchange step is followed by a final concentration step that results in a nominal concentration target of 0.5 to 1 mg/mL of encapsulated mRNA, which is a typical required concentration range for aerosol delivery. After concentration, the LNP formulation is subjected to 0.22 μm filter and stored frozen at −80 °C until use. The formulation characteristics can be found in supplementary material (*SI Appendix*, Table S1).

Wildtype Human Bronchial Epithelial Cell (WT hBEC) Culture. Human bronchial epithelial cells or hBECs (from a healthy nonsmoking donor) at passage 1 (P1) were obtained from University of North Carolina (UNC), Marsico Lung Institute Tissue and Procurement and Cell Culture Core. hBECs were expanded and a cell bank of P2 cells was generated by freezing down the expanded cells. For expansion, 60 mm plates were coated with collagen (PureCol®Type I Collagen Solution 3 mg/ml Bovine, Advanced BioMatrix # 5005) for 2 h at RT; cells were plated at 200,000 cells/plate in PneumaCult™-Ex Plus (Ex-Plus) Medium (Stem Cell Technologies #05040) and expanded until 80 to 90% confluency. After expansion, cells were detached using 0.25% trypsin and frozen down at P2 using 10% DMSO in Ex-Plus medium. For differentiation of hBECs in porous supports, frozen down cells at P2 were thawed and expanded. The expanded cells in the 60 mm plate were detached by treating the cultures with 0.25% trypsin for 10 min. Detached cells were counted and seeded on collagen coated inserts (Collagen from human placenta, Sigma #C7521) at 200,000 cells/insert (Transwell, Corning #3460 or Falcon, Corning #353104) in UNC-ALI medium (from University of North Carolina; Marsico Lung Institute Tissue and Procurement and Cell Culture Core). Cells were kept submerged for 72 h to allow expansion in inserts following which the apical medium was aspirated and cells were subjected to an ALI condition for differentiation. Medium in the wells was replaced with fresh UNC-ALI medium 3 d a week (M, W, F). After 10 d in ALI, cultures were washed with PBS (two washes of 5 min) each time before the medium change to remove an abnormal amount of excess mucus in a closed system. It is important to note that under these conditions a mucus layer remains present. For quality control, ciliary activity measurements were performed on day 21 post-ALI and before treatment. Cultures were considered well-differentiated at day 28 after ALI.

DNAI1-Knockdown (DNAI1-KD) hBEC Culture Model. The lentiviral transduction of WT hBECs for DNAI1 knockdown was done as described in (34) with modifications. Frozen hBECs at P2 were thawed at 37 °C. After resuspending the cells in Ex-Plus medium, cells were spun down at 150×*g* for 5 min and resuspended again in the same medium for a cell count. Lentiviral Transduction Particles with shRNA for knockdown of DNAI1 (Sigma # TRCN0000083441) were thawed on ice. A complex of hexadimethrine bromide at 2 μg/mL, virus at MOI4, and hBEC suspension was prepared, added to a collagen-coated 60 mm plate (at 200,000 cells/plate), and allowed to grow in a humidified CO_2 incubator at 37 °C with 5% CO_2. The following day, the virus containing medium was replaced with fresh Ex-Plus medium. The medium was replaced again 24 h later with fresh prewarmed Ex-Plus medium containing puromycin (1 μg/mL) for selection of transduced cells. Medium was changed every 48 h until the plate was 80 to 90% confluent. Cells were trypsinized and transferred to collagen coated porous membrane inserts as described above with UNC ALI medium containing puromycin at 2 μg/mL. Cells were kept submerged for 48 to 72 h to allow expansion in inserts following which the apical medium was aspirated to initiate differentiation. At ALI, cultures were initially maintained in PneumaCult ALI medium (from Stem Cell Technologies #05001) and slowly phased out to UNC-ALI over 10 d. Thereafter cultures were maintained in UNC ALI medium containing puromycin. During differentiation, medium in the wells was replaced 3 times a week (M, W, F). After 10 d in ALI, cultures were washed with PBS (two washes of 5 min each) at each time before the medium change to remove an abnormal amount of excess mucus in a closed system, however a mucus layer remains present. For quality control, ciliary activity measurements were performed on day 28 and before treatment. Cultures were considered well-differentiated at day 28 post-ALI.

LNP-mRNA Delivery using Vitrocell with Aerogen Solo Nebulizer. A temperature-controlled VITROCELL® CLOUD 12 System (Vitrocell) fitted with an Aerogen® Solo nebulizer (Aerogen Solo Nebulizer Kit;Tri-Anim, #06-AG-AS3000-US) was used for aerosol delivery of LNP-formulated mRNA to hBEC cultures. Before nebulization, the entire unit, except the lid and nebulizer, was UV sterilized for 30 min. During temperature equilibration, hBEC cultures (between 28 d to 45 d post-ALI) in Transwell inserts (Corning #3460) were washed with PBS on the apical side twice for 5 min each and rinsed with 300 μL of ultrapure water to remove excess mucus. Following the water rinse, cultures were nebulized within 15 min. Quantitative nebulization of LNP-formulated mRNA and aerosol cloud formation was completed in approximately 2 min. An additional 7 min was allowed to ensure complete settlement of the aerosol cloud before the culture inserts were placed back into their plate and returned to a 37 °C incubator. Treated cultures were rinsed with PBS 4 to 5 h after treatment to remove remnant formulation from the culture surface.

LNP-mRNA Delivery by Basolateral Treatment. hBEC cultures in Falcon inserts (Corning #353104) with pore size 1.0 μm were washed twice with PBS for 5 min each before treatment. Typically, formulations were diluted in the medium and 500 μL of medium was added to the wells of the plate. Cultures were incubated for 5 h, then the basolateral medium was replaced with fresh medium and cultures were placed back in the incubator.

WB Analysis. Prior to WB analysis, cells in inserts were rinsed with PBS and stored at -80 °C until processed. To extract total protein, 100 μL of RIPA (radioimmunoprecipitation assay) lysis buffer with 1% Halt protease inhibitor cocktail and 0.5% Universal nuclease was directly added to the apical side of the insert. Cells were incubated on a plate shaker for 15 to 30 min after which the lysates were spun down at 21,000×*g* for 10 min at 4 °C. The supernatant was transferred to a new tube, protein concentration determined with a BCA assay kit, and lysates stored at −80 °C until used.

For WB detection of DNAI1-HA protein, 7 to 10 μg of total protein per sample was separated on a 4 to 12% Bis-Tris SDS-PAGE gel (NuPAGE, ThermoFisher), transferred to a nitrocellulose membrane (ThermoFisher), stained for total protein using the Invitrogen No-Stain Protein Labeling Reagent (ThermoFisher A4449) following the manufacturer's instructions, and imaged using a Fluorchem M gel imager (Protein Simple). Membranes were then blocked with 5% nonfat milk in TBS (ThermoFisher) for at least 30 min and incubated with primary antibody overnight at 4 °C. A rat monoclonal anti-HA–HRP conjugate at a 1:2,000 dilution (Roche, 3F10) was used to detect DNAI1-HA protein. A rabbit monoclonal anti-DNAI1 antibody (Abcam, ab166912) at a 1:2,000 dilution and a secondary anti-rabbit IgG–HRP conjugate (ThermoFisher) at a 1:5,000 dilution was used for detection of endogenous mouse DNAI1. Blots were developed with SuperSignal West Femto chemiluminescent substrate (ThermoFisher) for 5 min at RT and imaged using a Fluorchem M gel imager (Protein Simple).

Ciliary Activity Measurement. For ciliary activity measurement, cultures in inserts were visualized individually using a Nikon Eclipse TE2000 inverted microscope with phase optics and a 20× objective (NA, 0.45). Using a Tokai HIT controller (model INU-TIZ-F1) and a microscope stage-heater block, the temperature of the cultures was maintained at 37 °C. High-speed videos (120 frames/s) were recoded using a Basler acA1300-200 μm camera controlled by SAVA software (Ammons Engineering). Ciliary activity is measured as "% active area" from one FoV (Fields of View; 20× magnification) using the SAVA software such that e.g. "40% active area" refers to 40% of the FoV surface area revealing detectable ciliary activity. CBF videos were analyzed using SAVA whole-field analysis with "G mean" column values reported. In WT hBEC cultures, 8 to 9 FoV were analyzed because ciliary activity is evenly distributed throughout the insert. In DNAI1-KD hBEC cultures, where activity can be lower and unevenly distributed, approximately 350 FoV per Transwell (112 mm diameter) or 60 FoV per Falcon inserts (33 mm diameter) were analyzed. FoV with % active area <0.1% were recorded as "0%." Prior to measurement, cultures were washed twice for 5 min with PBS to hydrate and remove excess mucus. Medium was replaced with appropriate fresh medium, and cultures were allowed to stabilize in a 37 °C incubator for 10 min.

Immunofluorescence and Quantification of Colocalized Cells. Whole-mount ALI cultures were washed briefly with PBS and 4% paraformaldehyde for 10 min. Cultures were washed 3 x 5 min to remove the fixative and permeabilized with 0.2% Triton X-100 in PBS (PBS-T) at RT. Cultures were incubated in blocking solution (1% BSA in 0.2% PBS-T) for 1 h at RT before staining with primary antibody in blocking solution overnight at 4 °C. Cultures were then incubated in fluorophore conjugated secondary antibody in blocking solution at RT for 1 h, washed 3 × 10 min with PBS-Tn and the nuclei stained using DNA dye Hoechst 33342 (Thermo Fisher Scientific). Insert membranes were mounted on slides with ProLong Diamond Antifade Reagent (Thermo Fisher Scientific). To improve imaging of DNAI1-HA protein incorporated into ciliary axonemes (Figs. 2 and 3), the fixation method was modified to remove cytoplasmic proteins as described in (35). Cultures were first washed with CSK buffer (100 mM NaCl, 300 mM sucrose, 3 mM $MgCl_2$, 10 mM PIPES, 0.25% Triton X-100, 5 mM EGTA) for 2 min at RT followed by fixation with 4% paraformaldehyde in CSK buffer for 10 min. After fixation, IF was carried out using an anti-acetylated α-tubulin and an anti-HA antibodies to label ciliated cells (AT+) and newly made DNAI1-HA protein (HA+), respectively. After imaging, ciliated cells were quantified using Zen Blue lite software; AT+/HA+ cells were quantified manually at 60x magnification. IF images were captured using a Zeiss Axio Observer Fluorescence Microscope. Exposure during imaging was normalized to secondary antibody only stained slides (negative control). All images were processed using Zeiss Zen Blue software.

Statistical Analysis. Statistical analysis was performed for two groups with Welch's *t* test or for multiple groups with one-way ANOVA by GraphPad Prism (ns = not significant, $P > 0.05$, $*P \leq 0.05$, $**P \leq 0.01$, $***P \leq 0.001$, $****P \leq 0.0001$).

Detection of DNAI1-HA and Cell-Type Specific Markers by Flow Cytometry. For biodistribution of DNAI1-HA in hBEC cultures after treatment with LNP-formulated *DNAI1-HA* mRNA, cells were analyzed using flow cytometry 24 h after administration. For processing cells, medium was aspirated, and the cell surface was washed once by 1× PBS. Cells trypsinized (0.25% Trypsin) for 15 min at 37 °C in a cell culture incubator. The digestion was quenched by adding equal volume of Defined Trypsin Inhibitor (Gibco) + 20% HIFBS (Gibco). Following detachment, cells were washed once by 1× PBS before fixing with 4% PFA in 1× PBS for 10 min at RT. Fixed cells were washed once by 1× PBS, and then permeabilized by eBioscience Permeabilization Buffer (Invitrogen) for 10 min at RT. After permeabilization, cells were blocked using 0.5% BSA + FcR Blocking solution (BioLegend) in permeabilization buffer for 30 min. Cells were then incubated with conjugated primary antibody cocktail for 60 min (*SI Appendix*, Table S2) in the dark at RT. Single color stain and no stain were used as controls. The CC10 antibody was conjugated with Alexa Fluor 488 in house using Alexa Fluor 488 Conjugation Kit (Fast)–Lightning-Link (Abcam). After primary antibody incubation, cells were washed once using 0.5% BSA in permeabilization buffer and once by flow running buffer (0.5% BSA in 1× PBS). Subsequently, cells were resuspended in 300 to 500 μL flow running buffer and analyzed using a SONY SA3800 Spectral Cell Analyzer.

Aerosol Exposure of Intubated NHP (In Vivo). All animal procedures were performed with ethical compliance and approval by the Lovelace Biomedical (Albuquerque, NM) Institutional Animal Care and Use Committee. LNP-formulated *DNAI1-HA* mRNA was aerosolized using an Aerogen® Solo nebulizer at Lovelace Biomedical. Ventilation was controlled by a Harvard pump. Ventilation settings were standardized at a tidal volume of 10 to 15 mL/kg of NHP body weight, 30 breaths per minute, and a 35:65 inspiratory to expiratory ratio. The aerosolized LNP-formulated *DNAI1-HA* mRNA was delivered to anesthetized animals through an endotracheal tube (ET, 4.5 mm inside diameter) with an inflated cuff placed into the trachea just beyond the laryngeal folds. A supply of 100% oxygen was provided through the breathing circuit. A two-way nonrebreathing Hans Rudolph valve was used to enable collection of exhaled test article on a box filter during dosing. The amount of aerosolized, LNP-formulated *DNAI1-HA* mRNA exiting the ET tube was estimated using preweighed glass fiber filter (47 mm GF/A filters, GE Whatman, Pittsburgh, PA) capture. The mRNA collected on the filters was quantified using both gravimetric and confirmatory chemical analyses using a RiboGreen® assay (Thermo Fisher Scientific). The filters were thoroughly dried at ambient conditions before weighing. Twenty to thirty second filter collections were performed in series before and after each NHP exposure. DD were estimated using DD (mg/kg) ≈ (M/t) * (T/BW) where M is the average (n = 2) *DNAI1-HA* mRNA mass deposited on filters, t the filter collection time, T the exposure duration, and BW the NHP body weight. Aerosol droplet size distributions were determined at the end of the ET by APS (Model 3321, Aerodynamic Particle Sizer, TSI Inc., Shoreview, MN) independently after the completion of the NHP dosing. Averaged MMAD and GSD of the aerosol are reported in Table 1.

Tissue Collection for Biodistribution Determination. During necropsy, the left lung from each animal was inflation fixed with 10% neutral-buffered formalin (NBF) and a total of eight 5 mm tissue sections were collected from the left caudal and cranial lobes capturing bronchi, large and small conducting airways, and alveoli. In addition, two 5 mm tissue samples were also collected from the trachea below the intratracheal tube cuff. Samples were fixed in 10% NBF for 24 h and then embedded in paraffin.

Multiplex Immunofluorescence (mIF). NHP lung tissue samples were analyzed using a multiplex immunofluorescence (mIF) biomarker panel. First, 4-μm-thick tissue sections were taken from each tissue block and mounted onto glass slides for mIF staining. Then, as a quality control check for the tissue samples, one slide from each selected sample was stained with hematoxylin and eosin and examined by a pathologist to confirm the presence of airway epithelial tissue. For the mIF analysis, one slide from each selected FFPE tissue block along with appropriate control slides were stained with the mIF panel antibodies (*SI Appendix*, Table S3) using a Leica Bond RX system using Opal dyes (Akoya Biosciences) for detection and scanned using a Vectra Polaris imager (Akoya Biosciences). Acquired images were then unmixed using InForm software (Akoya Biosciences) and imported into HALO image analysis software (Indica Labs) for analysis. To determine cell area, a nuclear expansion algorithm was used. The cytoplasm area was determined by expanding from the nuclear area, as determined by DAPI staining, 3 millimeters outward. The assigned nuclear and/or cytoplasm areas were then used to detect marker signal positivity and intensity. Next, a customized algorithm was used to calculate the single and HA-double positive cell populations across the whole slide.

MPPD Modeling. The MPPD (version 3.04) software was employed to simulate inhaled aerosol deposition patterns in NHP lungs using the symmetric Rhesus airway morphometry model (17, 18). While Mauritian cynomolgus or long-tailed

macaques (*Macaca fascicularis*) were used during in vivo administrations, phylogenetically closely related rhesus macaques (*Macaca mulatta*) were employed as NHP models implemented in MPPD for simulations.

Airway morphometry data in NHPs, i.e., FRC and URT volume, BF, and tidal volume (TV, the lung volume of air displaced by a typical inhalation and exhalation), are provided in (BW-dependent) default settings or can be manually entered as modeling parameters. MPPD input values employed in this study are summarized in Table 1.

Data, Materials, and Software Availability. All study data are included in the article and/or *SI Appendix*.

ACKNOWLEDGMENTS. We are grateful to Dr. Lawrence Ostrowski and Leslie Fulcher (Marsico Lung Institute) for initial guidance and protocols to establish primary human tracheobronchial epithelial cells (hBECs), prepared as described previously (PMID:2309104) and obtained under protocol #03-1396 approved by the University of North Carolina at Chapel Hill Biomedical Institutional Review Board, and Cystic Fibrosis Foundation Therapeutics (ESTHER24R0) and NIH (P30DK065988). We thank Dr. Lalithasri Ramasubramanian, Emmanuel Fasusi, and Alanna Manning for producing LNP-encapsulated mRNA formulations for in vitro studies, as well as Dr. Jackson Eby, Paul Gao, and Emily Howard for LNP-encapsulated mRNA formulations for in vivo studies. M.H. thanks Dr. Matthew Reed (CoelusBio) for fruitful discussions and Dr. Hammad Irshad and Derek Montoyo (Lovelace Biomedical) for aerosol exposures and analysis. This work was funded by ReCode Therapeutics.

Author affiliations: [a]Research and Development, ReCode Therapeutics, Inc., Menlo Park, CA 94025

1. M. Fliegauf, T. Benzing, H. Omran, When cilia go bad: Cilia defects and ciliopathies. *Nat. Rev. Mol. Cell Biol.* **8**, 880–893 (2007).
2. J. F. Reiter, M. R. Leroux, Genes and molecular pathways underpinning ciliopathies. *Nat. Rev. Mol. Cell Biol.* **18**, 533–547 (2017).
3. A. J. Shapiro *et al.*, Diagnosis, monitoring, and treatment of primary ciliary dyskinesia: PCD foundation consensus recommendations based on state of the art review. *Pediatr. Pulmonol.* **51**, 115–132 (2016).
4. J. Wallmeier *et al.*, Motile ciliopathies. *Nat. Rev. Dis. Prim.* **6**, 77 (2020).
5. K. A. Despotes, M. A. Zariwala, S. D. Davis, T. W. Ferkol, Primary ciliary dyskinesia: A clinical review. *Cells* **13**, 974 (2024).
6. W. B. Hannah *et al.*, The global prevalence and ethnic heterogeneity of primary ciliary dyskinesia gene variants: A genetic database analysis. *Lancet Respir. Med.* **10**, 459–468 (2022).
7. G. Pennarun *et al.*, Loss-of-function mutations in a human gene related to chlamydomonas reinhardtii dynein IC78 result in primary ciliary dyskinesia. *Am. J. Hum. Genet.* **65**, 1508–1519 (1999).
8. S. M. King, Axonemal dynein arms. *Cold Spring Harb. Perspect. Biol.* **8**, a028100 (2016).
9. Q. Rao *et al.*, Structures of outer-arm dynein array on microtubule doublet reveal a motor coordination mechanism. *Nat. Struct. Mol. Biol.* **28**, 799–810 (2021).
10. T. Walton *et al.*, Axonemal structures reveal mechanoregulatory and disease mechanisms. *Nature* **618**, 625–633 (2023).
11. M. E. J. Holwill "Dynein motor activity during ciliary beating" in *Cilia and Mucus, From Development to Respiratory Defense*, M. Salathe, Ed. (2019).
12. C. J. Woo *et al.*, Inhaled delivery of a lipid nanoparticle encapsulated messenger RNA encoding a ciliary protein for the treatment of primary ciliary dyskinesia. *Pulm. Pharmacol. Ther.* **75**, 102134 (2022).
13. L. E. Ostrowski *et al.*, Restoring ciliary function to differentiated primary ciliary dyskinesia cells with a lentiviral vector. *Gene Ther.* **21**, 253–261 (2014).
14. M. A. Zariwala *et al.*, Mutations of DNAI1 in primary ciliary dyskinesia. *Am. J. Respir. Crit. Care Med.* **174**, 858–866 (2006).
15. Q. Cheng *et al.*, Selective organ targeting (SORT) nanoparticles for tissue-specific mRNA delivery and CRISPR–Cas gene editing. *Nat. Nanotechnol.* **15**, 313–320 (2020).
16. A. S. Ramalho, F. Amato, M. Gentzsch, Patient-derived cell models for personalized medicine approaches in cystic fibrosis. *J. Cyst. Fibros.* **22**, S32–S38 (2023).
17. B. Asgharian, W. Hofmann, R. Bergmann, Particle deposition in a multiple-path model of the human lung. *Aerosol Sci. Technol.* **34**, 332–339 (2001).
18. B. Asgharian *et al.*, Development of a rhesus monkey lung geometry model and application to particle deposition in comparison to humans. *Inhal. Toxicol.* **24**, 869–899 (2012).
19. J. H. Sisson, J. A. Stoner, B. A. Ammons, T. A. Wyatt, All-digital image capture and whole-field analysis of ciliary beat frequency. *J. Microsc.* **211**, 103–111 (2003).
20. C. A. Boecking *et al.*, A simple method to generate human airway epithelial organoids with externally orientated apical membranes. *Am. J. Physiol.-Lung Cell. Mol. Physiol.* **322**, L420–L437 (2022).
21. R. E. Rayner *et al.*, In vitro 3D culture lung model from expanded primary cystic fibrosis human airway cells. *J. Cyst. Fibros.* **19**, 752–761 (2020).
22. T. Kato *et al.*, Reuse of cell culture inserts for in vitro human primary airway epithelial cell studies. *Am. J. Respir. Cell Mol. Biol.* **64**, 760–764 (2021).
23. K. J. Cho *et al.*, ZMYND10 stabilizes intermediate chain proteins in the cytoplasmic pre-assembly of dynein arms. *PLoS Genet.* **14**, e1007316 (2018).
24. N. T. Loges *et al.*, DNAI2 mutations cause primary ciliary dyskinesia with defects in the outer dynein arm. *Am. J. Hum. Genet.* **83**, 547–558 (2008).
25. A.-G. Lenz *et al.*, Efficient bioactive delivery of aerosolized drugs to human pulmonary epithelial cells cultured in air-liquid interface conditions. *Am. J. Respir. Cell Mol. Biol.* **51**, 526–535 (2014).
26. V. K. H. Bui, V. V. Tran, J.-Y. Moon, D. Park, Y.-C. Lee, Titanium dioxide microscale and macroscale structures: A mini-review. *Nanomaterials* **10**, 1190 (2020).
27. L. E. Ostrowski *et al.*, Conditional deletion of dnaic1 in a murine model of primary ciliary dyskinesia causes chronic rhinosinusitis. *Am. J. Respir. Cell Mol. Biol.* **43**, 55–63 (2010).
28. L. Guerra *et al.*, The preclinical discovery and development of the combination of ivacaftor + tezacaftor used to treat cystic fibrosis. *Expert Opin. Drug Discov.* **15**, 873–891 (2020).
29. T. Neuberger, B. Burton, H. Clark, F. V. Goor, Cystic fibrosis, diagnosis and protocols, Volume I: Approaches to study and correct CFTR defects. *Methods Mol. Biol.* **741**, 39–54 (2011).
30. I. A. L. Silva, O. Laselva, M. Lopes-Pacheco, Advances in preclinical in vitro models for the translation of precision medicine for cystic fibrosis. *J. Pers. Med.* **12**, 1321 (2022).
31. P. G. Czarnecki, J. V. Shah, The ciliary transition zone: From morphology and molecules to medicine. *Trends Cell Biol.* **22**, 201–210 (2012).
32. E. Toskala, S. M. Smiley-Jewell, V. J. Wong, D. King, C. G. Plopper, Temporal and spatial distribution of ciliogenesis in the tracheobronchial airways of mice. *Am. J. Physiol.-Lung Cell. Mol. Physiol.* **289**, L454–L459 (2005).
33. X. Wang *et al.*, Preparation of selective organ-targeting (SORT) lipid nanoparticles (LNPs) using multiple technical methods for tissue-specific mRNA delivery. *Nat. Protoc.* **18**, 265–291 (2023).
34. N. Baumlin-Schmid, M. Salathe, N. L. Fregien, Optimal lentivirus production and cell culture conditions necessary to successfully transduce primary human bronchial epithelial cells. *J. Vis. Exp.* **22**, 113 (2016).
35. K. Hua, R. J. Ferland, Fixation methods can differentially affect ciliary protein immunolabeling. *Cilia* **6**, 5 (2017).